INTERNATIONAL JOURNAL OF COMMUNICATION SYSTEMS
Int. J. Commun. Syst. 2008; **00**:1–6 *Prepared using* dacauth.cls *[Version: 2002/09/18 v1.01]*

Performance of Markov models for frame-Level errors in IEEE 802.11 wireless LANs

Gennaro Boggia *, Pietro Camarda, and Alessandro D'Alconzo

Dipartimento di Elettrotecnica ed Elettronica - Politecnico di Bari. Via Orabona, 4 – 70125 Bari, Italy.
(e-mail:{g.boggia,camarda,a.dalconzo}@poliba.it)

SUMMARY

Interference among different wireless hosts is becoming a serious issue due to the growing number of Wireless LANs based on the popular IEEE 802.11 standard. Thus, an accurate modeling of error paths at the data link layer is indispensable for evaluating system performance and for tuning and optimizing protocols at higher layers. Error paths are usually described looking at sequences of consecutive correct or erroneous frames and at the distributions of their sizes. In recent years, a number of Markov-based stochastic models have been proposed in order to statistically characterize these distributions. Nevertheless, when applied to analyze the data traces we collected, they exhibit several flaws.

In this paper, to overcome these model limitations, we propose a new algorithm based on a semi-Markov process, where each state characterizes a different error pattern. The model has been validated by using measures from a real environment. Moreover, we have compared our method with other promising models already available in literature. Numerical results show that our proposal performs better than the other models in capturing the long-term temporal correlation of real measured traces. At the same time, it is able to estimate first order statistics with the same accuracy of the other models, but with a minor computational complexity. Copyright © 2008 John Wiley & Sons, Ltd.

KEY WORDS: Frame error process, measured data analysis, channel modeling, Markov models

1. Introduction

Nowadays, as we can seen in a lot of communication applications, the popularity of 802.11-based Wireless LANs (WLANs) is growing. As a consequence, the ever increasing interference level among transmitting systems could impair their overall performance. Together with the strict requirements of real-time applications (e.g., audio and video streams), this will stress the capability of the current WLANs.

It is well known that wireless links are much more error prone, than the traditional wired ones, either with respect to bit and frame error rates. However, the most challenging problem is that errors occur in a bursty fashion, i.e., there are long periods of correct transmissions

*Correspondence to: G. Boggia

Contract/grant sponsor: Apulian Region Projects PS-121

Received XXXXXX
Revised XXXXX

spaced with short periods during which the communication is strongly affected by bit errors and, then, by losses/corruption of frames and/or packets. This is mainly due to the fading mechanism, intersymbol interference, multipath propagation, and interference phenomena [1].

On the other hand, since communication protocols at the higher layer operate on the basic unit of a frame or a packet, the modeling of error paths at the data link layer is of particular interest. This also simplifies the study of the effect of errors on the higher layers. However, the channel coding in a transmission system greatly affects the error distribution properties, and, at the same time, code performances are limited by error distribution. Therefore, we are interested not only in the average number of errors, but rather in the whole error distribution (or at least in the knowledge of some statistical moments) and in its temporal correlation structure.

The characterization of errors at the frame-level is not a trivial issue and many research efforts were addressed in this direction in recent years (e.g., [2]-[5]). In fact, the accurate wireless channel modeling at the link layer is indispensable for evaluating system performance and for tuning and optimizing communication protocols interaction at higher layers [6]-[8].

As extensively reported in Section 2, even though several approaches are possible to model wireless channels, in this paper we focus on measurement based stochastic models. In particular, we consider the important subclass of Markov-based models, due to their ability to fit various error behaviors and to keep low computational complexity.

Starting from measures collected in a 802.11 WLAN, performance of several Markov-based models have been analyzed. We considered some promising Markov models for describing frame-level errors in wireless channels, that is, the Extended ON/OFF model [3], the MTA [6] and the M^3 [9], and the well-known k-order Finite State Markov Chains (FSMCs). We studied the validity of such models for the considered real data traces, referring, in particular, to their capability in capturing the long-term autocorrelation structure of frame error traces which importance has been highlighted in [3].

We found that such models do not perform well in fitting the autocorrelation function of the error distributions. To overcome this shortcoming, we propose a new scheme, henceforth referred to as *k-state threshold model*, which is the generalization of the ON/OFF logarithmic model [10], already successfully applied to analyze the frame error trace on a GSM wireless channel. The k-state threshold model is a semi-Markov [11] model, where in each state different error paths are generated by using different distributions for both error and error-free burst lengths. Its parameters are estimated from data traces by using the Maximum Likelihood method [12]. This model was developed with the aim to keep low the computational complexity; in fact, it requires the estimation of only few distribution parameters.

The rest of the paper is organized as follows. A comprehensive discussion of related works is reported in Sec. 2. The test bed and the data analysis are described in Sec. 3. In Sec. 4, models considered for the comparison with our approach are illustrated. Sec. 5 shows our proposal. Model validation and performance are discussed in Section 6. Finally, in Sec. 7 conclusions and future work are outlined.

2. Related Works

To analyze wireless channel error, several approaches are possible: there are deterministic and stochastic models. Theoretically, it is possible to achieve a detailed deterministic description

of a communication channel at the physical layer by means of, as an example, the ray tracing techniques [13]. In this case, it requires a large amount of rays, the knowledge of the electromagnetic behavior of the environment (reflectivity, absorption), and so on. But such descriptive models are unsuitable to represent channel behavior in computer simulations when also higher layers are considered, due to the wasteful computational overhead. Moreover, some of the error sources in wireless communication are intrinsically stochastic (e.g., thermal noise). Thus, in general, all the relevant error models are stochastic.

Stochastic models consider the analysis of the *bit (frame) error trace* [3], which is a binary sequence of 0's and 1's: every bit of the trace represents the state of a received bit (frame). In particular, a bit is 0 if the bit (frame) has been correctly received, otherwise it is 1. An *error burst* is defined as a run of consecutive 1's, as well as an *error-free burst* is a run of consecutive 0's. Given that in this paper we are interested in the data-link layer behavior, in the following, unless stated otherwise, we will refer to frame error traces.

As Markov systems are very well known and have many useful proprieties, they have been widely applied to describe various channel characteristics. In this large family of models, there are approaches that try to represent some physical characteristics as well as approaches that disregard any physical meaning.

Further distinguishing, some Markov-based models relay on some physical channel description (e.g, Amplitude-based Finite State Markov Chains, AFSMCs) whereas many others refer to experimental data. In AFSMCs, a finite number of states is used either to represent the amplitude envelope of the received signal or to characterize SNR variations. They are employed to generate successive events (fade levels) that, in general, may be correlated. In [14] and [15], a first-order Markov chain has been considered with the assumption of a Rayleigh fading channel. Instead, in [16] higher order Markov chains are used to model correlated Rician-fading channels. In [17], AFSMCs have been found to be appropriate for characterizing the SNR variations in slow fading channels. In [18], such an approach has been extended also for modeling frame losses. However, no validation of this model against experimental data coming from WLANs has been performed. Furthermore, these and other studies have assumed that the underlying communications channel is not frequency selective (assumption valid only for narrowband channels), and that fairly simple modulation schemes are being used. These assumptions are not valid for wideband channels like those ones used by 802.11 devices.

Focusing on Markov models for digital channels, a traditional approach to link-layer error modeling is the use of Finite State Markov Chains (FSMCs). Since the states are observable, the great advantage of these models is that we can obtain the state probability vector and the transition probability matrix by computing directly the frequency of transitions occurring in the frame-error trace. Moreover, it is possible to derive closed form solutions for most performance metrics. The simplest FSMCs, referred to as Gilbert [19, 20] and Gilbert-Elliot models [19] (i.e., two-state discrete time Markov processes), have been used to study the error behavior in wired links, but they do not produce accurate results in wireless environment [5]. Therefore, the Improved Two-State model was developed [20], but results obtained with this simple Markov model has been proved to be not suitable to represent even GSM cellular error traces.

In Hidden Markov Models (HMMs), a proper probability function is built over the state space embedding the observable stochastic process. Although the use of HMMs improves model capability to emulate the statistical properties of a real system, it leads to a dramatic increase of computational complexity, due to the estimation of model parameters using algorithms such

as the Baum-Welch one [21], [22]. Moreover, in [7] and [23], it has been proved that high order HMMs are unsuitable even for a WLAN environment. In spite of the increasing complexity, there is not a consistent improvement of all the performance metrics.

Recently, several new models have been proposed to overcome these limitations. The GAP model [19] adopts a time-inhomogeneous Markov chain to fit distributions of error and error-free burst lengths. The Bipartite model [24], instead, gives better approximation of the packet error correlation over longer timescales than other models, but such an algorithm is quite complex because it requires the estimation of a huge number of parameters. Another interesting approach is the one that used Chaotic Map models [25]; they are particularly suitable for matching error/error-free burst distributions with extremely long-tails. For this reason, they have been exploited only to study errors at bit level rather than at frame level when error traces do not show such a long tail behavior.

Finally, in the data preconditioning framework for GSM wireless systems [6, 9], two new models, referred to as Markov-based Trace Analysis (MTA) [6] and M^3 model [9], have been proposed. Recently the ability of such models in capturing some important second order trace statistics has been brought into question in [3], where authors propose the Extended ON/OFF model to explicitly address this issue.

Since the latter two approaches seem to be the most promising ones and have been already fruitfully applied in modeling wireless links, they are considered for the comparison with our new proposal. Thus, further details about both these approaches are given in Sec. 4.

Note that the Bipartite model is complex and requires the estimation of a very huge number of parameters (even hundreds) to achieve an acceptable level of accuracy. For this reason, such a model is not considered in our comparison section. Moreover, also the comparison with Chaotic Map is not reported because it has been conceived for modeling errors at bit level, but we are interested in errors at frame level, and because in this paper our attention is devoted to Markovian models. However, as discussed in the conclusions, in future work we will consider a comparison of our scheme with Chaotic Maps applied to error traces at frame level.

3. Data Collection and Analysis

Wireless LANs are generally plug-and-play in nature and are being purchased not just by network administrators, but also by families to share internet broadband access, by shop owners, and so on. As a consequence, unlike cellular systems where base-stations are strategically placed, WLAN Access Points (APs) are deployed blindly. This causes, in complex WLAN environment, that coverage areas of different APs overlap, generating mutual interference; i.e., we can have in the same area more WLANs using the same (or close) frequencies with high interference.

In order to get an insight into the frame error process for such a scenario, we settled down, in a typical indoor environment, the test bed shown in Fig. 1. The idea was to realize sniffing session of controlled transmissions from a Traffic Generator (TG) software, in presence of induced radio interference on the transmission channel. Two different WLAN are realized with two different APs; the laptop computers are equipped with a wireless network interface card.

The laptop computer associated to AP 1 and the workstation in Fig. 1 realize the useful communication, from which the frame traces are obtained by using another laptop computer with a wireless traffic sniffer.

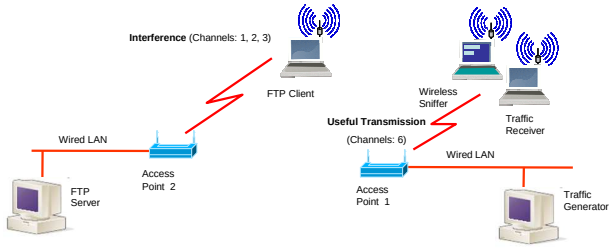

Figure 1. Experimental scenario for obtaining measurements.

A workstation acting as a FTP server and a laptop computer acting as client (equipped with a wireless network interface card and associated to the AP 2) realize the interference transmission. We considered an FTP traffic because as it tries to use the maximum available bandwidth, it maximizes the interference level in the considered area.

While collecting frame error traces, we have considered different measurement scenarios. A different traffic flow for the useful transmission and a different radio channel for the interference transmission have been exploited. In particular, we have generated a G-729A coded [26] voice stream (henceforth referred to as VoIP traffic) and an UDP traffic with constant size datagrams (512 bytes) at three Constant Bit Rates: 128, 256, and 512 kbps. For what concerns the radio channels for the interference transmission, we used channels 1, 2, and 3 (i.e., according to 802.11 standard [27], the radio channels with a bandwidth of 22 MHz and carriers at 2.412 GHz, 2.417 GHz, and 2.422 GHz, respectively). The useful transmission is always realized on the radio channel 6 (i.e., with carrier at 2.437 GHz).

We highlight that changing the interference channel we consider different WLAN scenarios. In fact, when the interference is on channel 1, the scenario is realistic and it corresponds to a well planned WLAN with a proper frequency reuse, that is with a gap of five frequencies between adjacent channels (e.g., channels 1-6-11). Instead, when the interference is on channel 2 or 3, we are considering in any case a realistic scenario with several WLANs sharing the same area without coordination. Such a scenario is getting more and more realistic in an urban environment.

Using the described measurement test bed, ten frame-error traces were collected for each traffic flow and interference channel, obtaining overall 120 different traces, each one 4 minutes long.

3.1. Analysis and Characterization of Frame Error Traces

Let Z_i be the sequence of random variables corresponding to the frame error trace, i.e., $Z_i = 1$ in presence of an error frame, $Z_i = 0$ otherwise. Let X_R and X_F be the random variables of the lengths of error and error-free bursts, respectively. Let $\overline{x}_R$, $\overline{x}_F$, and σ_{X_R}, σ_{X_F}, be their means and standard deviations, respectively. To characterize the collected frame error traces we consider:

- the *Frame Error Rate (FER)*:

$$FER = \overline{Z} = \overline{x}_R/(\overline{x}_R + \overline{x}_F) \; ; \tag{1}$$

- the *Complementary Cumulative Distribution Functions* (CCDFs) of X_R and X_F:

$$\Psi(x_R) = P(X_R > x_R), \qquad \Phi(x_F) = P(X_F > x_F); \tag{2}$$

- the mean length, the standard deviation, and the coefficient of variation (i.e., the ratio between standard deviation and mean) of Error and Error-free bursts;
- the *autocorrelation coefficient* calculated by the well known estimator [12]:

$$\rho_Z(h) = \left(\frac{1}{n-h} \sum_{i=1}^{n-h} (Z_{i+h} - \overline{Z})(Z_i - \overline{Z}) \right) \Bigg/ \left(\frac{1}{n} \sum_{i=1}^{n} (Z_i - \overline{Z})^2 \right), \tag{3}$$

where n is the number of samples and h is the lag expressed in frames.

Considering the correlation coefficient as metric is important because a key point of this work is the analysis of the correlation structure of error and error-free bursts. In fact, as already mentioned and as stated in other papers (e.g.,[3, 10]), it is important to capture how error and error-free bursts succeed one to each other in the time.

In Fig. 2, measured mean FERs for each interference scenario and traffic flow are reported. Results are not surprising: the mean FER increases with the interference level. There is the same trend as the transmission rate of traffic flows increases. In particular, we can see that channel separation has more influence on FER than flow data rate.

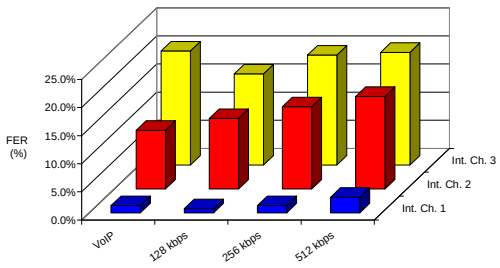

Figure 2. Mean FER in different interference and transmission conditions.

From Fig. 3, it can be noticed that the mean length of error bursts rises with the interference level and the transmission rate. On the other hand, the mean length of the error-free burst (i.e., the duration of error-free transmissions) becomes shorter as the interference level becomes non negligible (see Fig. 4). Nevertheless, the mean error-free burst length shows great variation, as the transmission rate varies, only when the interference level is negligible (i.e., interference on channel 1), but the same does not happen in presence of higher interference levels.

Figs. 5 and 6 show the mean value of the Coefficient of Variation (CoV), for the length of error and error-free bursts, as a function of the interference channel and the transmission rate. The CoV for error burst length is always smaller than 1 (i.e., the CoV of an exponential distribution), whereas the CoV for length of error-free bursts is always greater than 1 and sometimes close to 2, which means that there is a great error-free burst length variability.

Such a variability justifies the need for an analysis of second order statistics. To this aim, as already highlighted in [3], it is important to consider the measure of the autocorrelation coefficient. The analysis of the autocorrelation for measured data points out some important

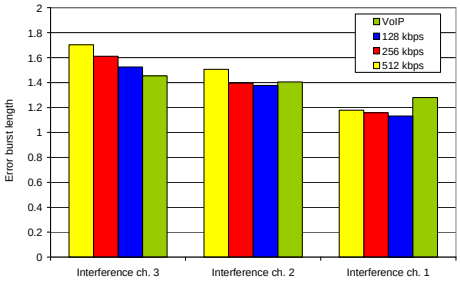

Figure 3. Mean length of Error burst.

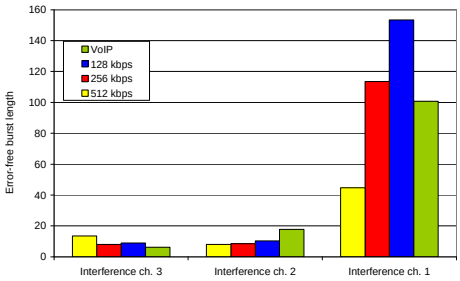

Figure 4. Mean length of Error-free burst.

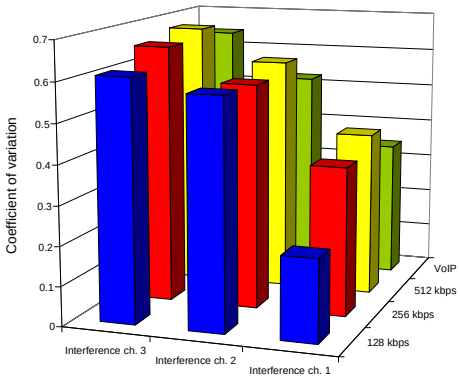

Figure 5. Mean variation coefficient of error burst length.

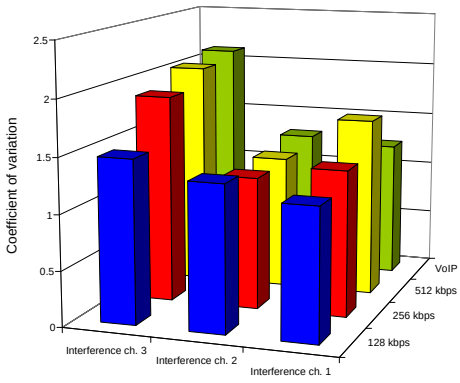

Figure 6. Mean variation coefficient of error-free burst length.

peculiarities concerning randomness of errors in frame traces. As an example, in Fig. 7 the autocorrelation coefficients of three VoIP transmissions (obtained under changing interference conditions) and the confidence bound at the significance level[†] $\alpha = 0.01$ (shown as dashed line) have been depicted. This allows us to assess the time scale over which temporal correlation assumes values significantly different from zero. The use of confidence bound is important because we cannot arbitrarily establish when correlation is small, but we can state that correlation is negligible if it is under the confidence bound.

From Fig.7, it is evident that an increase of interference leads to a higher correlation level. Specifically, for traces collected when the interfering signal was on channel 1, the autocorrelation decays to zero into ten frames. On the other hand, when interference was on channels 2 and 3, samples are significantly correlated over longer time scale (i.e., in the range of $10^2 \div 10^3$ frames). A similar behavior has been noticed for transmissions obtained in the same interference conditions, but changing the source transmission rate (i.e., from 128 kbps to 512 kbps). In these cases, the correlation rises as the transmission rate increases; moreover, the time scale over which dependence decays to zero tends to increase. This behavior could

[†]For details about calculations of confidence bounds, see [28].

be easily explained considering that, increasing the transmission rate, neighboring samples are affected by similar fading conditions, so that the erroneousness or the correctness of received frames are closely correlated.

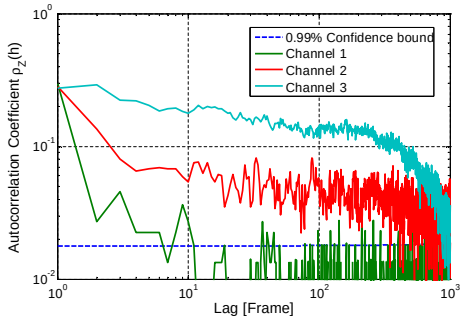

Figure 7. Autocorrelation coefficient of VoIP transmissions in presence of different interference conditions.

This analysis of frame error traces confirms that indoor wireless channels cannot be easily characterized. Therefore, our measurements can be useful in developing more accurate models. Finally, the analysis points out the needing of models which accurately capture not only the FER of traces and the error/error-free burst distributions, but also the long term temporal autocorrelation structure of the error paths. In fact, as both higher speed traffic sources and higher interference level are expected for WLANs, the long term temporal correlation structure of error paths will be further stressed.

4. Markov Models for Frame Loss Process

As known, some recent papers proposed and evaluated models for frame-level errors [3, 9] (in particular, in GSM channels). Herein, we want to assess their performance in modeling the collected 802.11 error traces. In this section the *k-th-order FSMC* models, the two models based on the *data preconditioning* technique [9], referred to as the *MTA* and the M^3 models, and the *Extended On/Off Model* [3] have been reviewed. In particular, we show how to apply such models to fit our measured error traces.

4.1. K-th-order FSMC models

We start by reviewing the well known *k-th-order FSMC* models, already fruitfully exploited in characterizing packet losses in wired links. These models are also the starting point for the data preconditioning techniques.

Let $\{S_n, O_n\}_{n=1}^{\infty}$ be a stochastic process, where $\{S_n\}$ is the sequence of states associated with a k-th order finite state discrete time Markov chain, with transition probability matrix $A = [a_{ij}]$ and asymptotic probability state vector $\Pi = [\pi_j]$; $\{O_n\}$ is the sequence of outputs generated by the Markov chain.

In our context, the state space is $\mathcal{S} = \{0, 1\}^k$ and the generic state S_n is a chunk of k elements taken from the frame error trace; that is, there are 2^k possible states and we can find

the sequence $S_n = (s_{1,n}, s_{2,n}, \dots s_{k,n})$, with each $s_{i,n} \in \{0, 1\}$, in the frame error trace. Each output O_n represents the k-th element of the sequence S_n in the error trace and, therefore, can assume only the following values: 0 or 1.

Let $P[O_n = 1|S_n] = b_i$ and $P[O_n = 0|S_n] = (1 - b_i)$ be the probabilities that the output of the Markov process is 1 or 0, respectively, when in the state S_n. Obviously, it follows that $b_i = s_{k,n}$, i.e., we have the output O_n equal to 1 with probability 1, if the last frame of the sequence S_n in the error trace is 1, otherwise the output $O_n = 1$ occurs with probability 0.

Considering the two states $S_n = (s_{1,n}, s_{2,n}, \dots s_{k,n})$ and $S_m = (s_{1,m}, s_{2,m}, \dots s_{k,m})$ of the k-th-order Markov chain, the transition from S_n to S_m may occurs only if $s_{i,m} = s_{i+1,n}$, for each $i = 1, \dots, k-1$. Thus, it is possible to derive the transition matrix A from a given error trace simply counting the number of transitions from sequence S_n to S_m. In the same way, the state probability vector Π is obtained counting how frequently each sequence appears in the trace. Obviously, the computational complexity of such a procedure increases with the order k of the Markov model, which also defines the memory length of the FMSC.

In [8], the choice of k is based on the autocorrelation analysis; whereas in [29], it is based on the concept of *conditional entropy*. Other approaches based on entropy have been already fruitfully exploited in [4] and [18].

Herein, considering [29], we propose the following technique that, in our opinion, gives a more objective methodology. Let $[z_1, z_2, \dots, z_n]$ be a sequence taken from the frame error trace; we can consider it as a realization of the stochastic process related to the set of random variables $Z_1, Z_2, \dots, Z_n$. From a source-coding perspective, the *joint entropy* $H(Z_1, Z_2, \dots, Z_n)$ provides the measure of the minimum number of bits necessary to uniquely represent all the possible outcomes of the sequence. Moreover, if the random variable W represents the next element of the trace, the *conditional entropy* of order n, $H(W|Z_1, Z_2, \dots, Z_n)$, is an indication of the randomness of the next element in the trace, given n steps of the past history. From the information theory, it is known that $H(W|Z_1, Z_2, \dots, Z_n)$ is decreasing with n. Thus, a measure of the goodness of trace approximation by a k-th-order Markov model, could be expressed by:

$$\min_k \left(\frac{H(W|Z_1, Z_2, \dots, Z_k)}{H(Z_1, Z_2, \dots, Z_k)} < \epsilon \right) \tag{4}$$

where ϵ is a suitable value smaller than 1.

That is, the best choice for k is obtained considering the minimum value which ensures a ratio between conditional and joint entropy below a given threshold ϵ, i.e., when the amount of further information carried by the $(k+1)$-th element, given k past elements, becomes negligible. Obviously, lower values for ϵ results in higher values for k. Considering our measured traces, we found that $\epsilon = 0.2$ is a suitable choice for maintaining reasonably low the order k of the Markov models; in particular, with this choice we obtained for k values in the range $4 \div 5$, (i.e., models with $16 \div 32$ states).

4.2. Data preconditioning models

In [9], the authors propose a technique which consists of analysis and preconditioning of data before they are fed into traditional Markov models. Using pattern recognition, datasets are divided in subtraces which experience stationarity behavior. Each frame-error trace is divided into *lossy* and *lossy-free periods*. The lossy periods are concatenated to form the lossy subtraces, while the error-free periods are concatenated to form the error-free subtraces.

Therefore, the MTA (Markov-based Trace Analysis) algorithm proceeds identifying two states, one for each subtrace, and modeling the lengths of lossy and lossy-free frame sequences by two geometric distributions. Finally, the lossy subtrace is modeled by using a k-th-order FSMC (as shown above in Sec. 4.1), as well as the error-free state is modeled by a process which always outputs 0.

Unlike the MTA, the M^3 (Modified hidden Markov Model) algorithm is capable of modeling traces with non-exponential state length distributions. Similarly to a HMM, the M^3 considers each data subset as coming out from a hidden state. It models not only states, but also transitions among states, with high order FSMCs. That is, using the M^3 algorithm for our goal, we model the lossy subtrace by a FSMC of order k_{lt} (again with the technique described in Sec. 4.1), the lossy-free subtrace by a process which always outputs 0, and transitions between an error-free subtrace and a lossy subtrace by another FSMC of order k_{hs}, which states are referred to as hidden states.

4.3. The Extended ON/OFF model

In [13], Ji et alt. show that a GSM frame-level error process can be described by a discrete time two states (ON/OFF) semi-Markov model with the holding time of each state characterized by a mixture of geometric distributions.

The procedure provides a scheme for obtaining the parameters of geometric distributions and their relative weights in the mixture, by fitting the CCDFs of error and error-free burst lengths. Nevertheless, to improve model performance, the Expectation Maximization (EM) procedures is applied following the Baum-Welch algorithm [21]. The drawback is that this iterative optimization technique heavily increases the computational cost of the Extended ON/OFF model, as it involves a number of computations (for each iteration step) in the order of $O(k^2N)$ [21], where k is the total number of geometric distributions and N is the training sequence length (that is, the frame error trace length). Since the Extended ON/OFF method supplies a starting guess point for the EM optimization procedure, either the number of iterations and the computational cost cannot be easily foreseen. Thus, the computational cost of the Extended ON/OFF model may dramatically grow with the number of model states or the training sequence length.

We have applied such a model to describe the collected 802.11 error traces. In order to make a comparison with the other models and to keep low computational costs, we have chosen a suitable number of geometric distributions for each state. In particular, for modeling the OFF state always one geometric distribution has been used, whereas for the ON state a mixture of two or three geometric distributions have been used. These choices are motivated by the discussion about error and error-free burst length distributions that we have reported in Sec. 3. In fact, as the error burst lengths show small values for mean and variance, one geometric phase is a suitable choice for the OFF state; whereas, to model error-free burst lengths, which show greater variance, more geometric phases are needed.

5. The k-state Threshold Model

A comprehensive performance comparison of the models described above will be reported in Sec. 6. It will be shown that such models are not satisfactory in capturing the long-term

autocorrelation structure of 802.11 frame error traces. This task is not trivial and it is the goal of our model which will be described in this section. It is referred to as *k-state threshold model* (k-TM).

Note that it is not simple to capture second order statistics of frame error traces, whereas it is possible to estimate first order statistics (e.g., FER and CCDF) with good accuracy using simple models. As an example, we can consider a simple two-state (ON/OFF) semi-Markov model for analyzing our data. An error burst is generated when the system is in the OFF state, whereas an error-free burst is generated when in the ON state. Let X_R and X_F be the two random variables representing error and error-free burst lengths, respectively. We can estimate their CCDFs, $\Phi(X_R)$ and $\Psi(X_F)$, (i.e., the empirical stepwise distribution functions for error and error-free burst lengths) directly from the frame traces (see eq. 2). Now, using $\Phi(X_R)$ and $\Psi(X_F)$, we can generate a synthetic trace with the same first order statistics of the data. Nevertheless, comparing the autocorrelation coefficient of such a synthetic trace with the one of the data trace (see Fig. 8), results are very different. This show that the simple ON/OFF model is not able to preserve the temporal structure of the trace: that is, how error and error-free bursts follow one another.

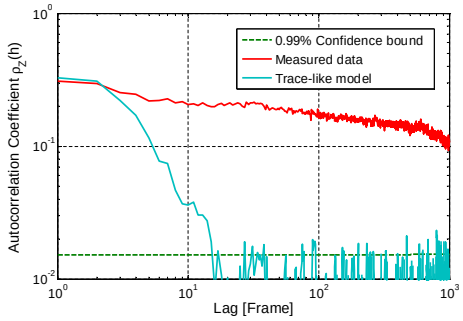

Figure 8. Comparison of the autocorrelation obtained by measured data and by considering a simple ON/OFF model.

As intuition suggests, when long error-free burst occurs (i.e., the quality of the received signal is quite good), it is likely that error frames occur either sporadically or in very short bursts. On the other hand, when the transmission channel conditions get worst, error-free bursts will be shorter and error frames will occur often and clustered in longer bursts. To capture such a temporal structure, we propose our new k-TM scheme based on a semi-Markov chain with k states ($k > 1$) as defined below. Since, the analysis of the error-free burst length in Sec. 3 pointed out the great variability of such a value (i.e., it ranges from one frame up to thousands of frames), our idea was to characterize model states with respect to the size of error-free bursts.

Let $T^{(k)}$ be a set of $k-1$ thresholds ϑ_i in the range of the error-free burst lengths:

$$T^{(k)} = \{\vartheta_i \mid 1 \leq \vartheta_i \leq M_{EF};\ \vartheta_i < \vartheta_j,\ i < j;\ 1 \leq i, j \leq k-1\}; \tag{5}$$

where M_{EF} is the maximum value for the lengths of error-free bursts.

Let $\Omega = \{F_n, R_n\}_{n=1}^{\infty}$ be the ordered sequence of error-free bursts, F_n, and error bursts, R_n, as they appear in the data trace.

Given the $k-1$ thresholds, we are in the state S_i if we observe in the data trace error bursts $\{R_n\}$ and error-free bursts $\{F_n\}$ that satisfy the following conditions:

$$F_n \in S_i \text{ if } \begin{cases} x_{F_n} \leq \vartheta_1, & i = 1; \\ \vartheta_{i-1} < x_{F_n} \leq \vartheta_i, & 1 < i \leq k-1; \\ x_{F_n} > \vartheta_{k-1}, & i = k \end{cases} \qquad R_n \in S_i \quad \text{if } F_{n-1} \in S_j, \;\; j \geq i; \tag{6}$$

with x_{F_n} and x_{R_n} lengths of the burst F_n and R_n in state S_i, respectively; F_{n-1} is the error-free burst which immediately precedes the error burst R_n.

In other words, an error-free burst belongs to the state 1 if its length is less than ϑ_1, or to the state i if its length is in the range $(\vartheta_i - 1; \vartheta_i]$, or to the state k if its length is greater than ϑ_{k-1}. On the other hand, an error burst belongs to a generic state i if it follows an error-free burst either of the same state i, or of a state j but with $j \geq i$.

Hence, when an error-free burst occurs in state S_i, the model is in the ON phase of S_i. Similarly, when an error burst occurs in state S_i, the model is in the OFF phase of S_i. The above equations state that (see Fig. 9): from an ON phase S_i, system can switch only in the OFF phase of the same state or of a previous state; from an OFF phase in S_i, system can switch only in the ON phase of the same state or of a successive state.

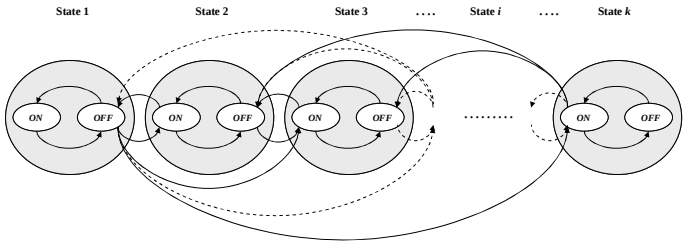

Figure 9. State diagram of k-TM model.

In the model, $\Psi_i(x_R)$ and $\Phi_i(x_F)$ are the CCDFs of the lengths of error and error-free bursts in S_i, respectively.

The sojourn time in S_i (i.e., the sum of the time spent in both the ON and OFF phases of state i) is characterized by the CCDF $\Upsilon_i(n_b^i)$ of the discrete random variable N_b^i which counts how many error and error-free bursts occur when in the given state.

Transitions among states are governed by and by the $k \times k$ transition probability matrix $\mathbf{P}$, which each element $p_{ij} = p(S_i|S_j)$ is the probability to transit from S_i to S_j. Note that $p_{ii} = p(S_i|S_i) = 0$ because, once the sojourn time in S_i expires, the system must jump to another state.

Moreover, the state probability vector $\mathbf{\Pi} = \{\pi_1, \ldots, \pi_k\}$ defines the occurrence probabilities of each state.

5.1. Estimation of model parameters from data traces

The threshold model defines a general framework, since the distribution functions have to be characterized in order to fit real data. In the following, we will show how to apply the proposed approach to our measured data set, choosing the appropriate fitting distributions for $\Phi_i(x_F)$, $\Psi_i(x_R)$, and $\Upsilon_i(n_b^i)$ for each i. Moreover, we describe how to estimate $\mathbf{P}$ and $\mathbf{\Pi}$.

To keep low the model complexity and to make a fair comparison with the other Markov models presented in this paper, we will consider only the simplest case of $k = 2$, i.e., only one threshold. Also with this assumption, we will show that our model works well. However, the effectiveness of the k-TM scheme can be further improved considering more states.

For sake of simplicity, we will refer to the two states of the model, S_1 and S_2, as *Above threshold* and *Below threshold* states. Accordingly to model definition, in both the two states, when the model is in the ON phase an error-free burst is generated, otherwise in the OFF phase an error burst is generated.

Since the threshold model has been conceived with the aim of capturing the temporal autocorrelation of frame error traces, the set $T^{(k)}k$ is chosen in order to minimize the mismatch between data and model autocorrelation. When in the presence of only one threshold, the data trace is split in two sub-traces by using Eq. (6). In Fig. 10 an example of the application of the aforesaid procedure in the case of threshold $\vartheta_1 = 5$ is illustrated.

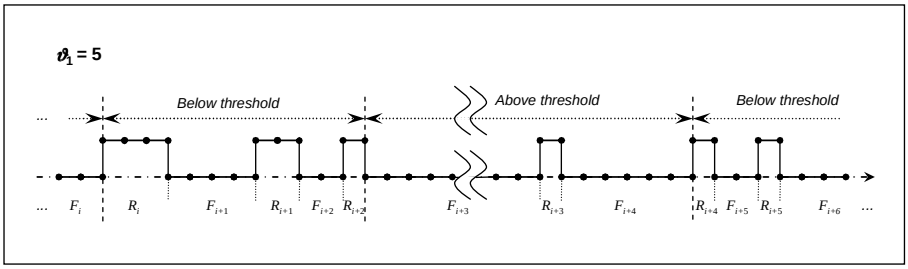

Figure 10. Time diagram for the threshold model with two states.

It is worth noticing that system always reaches/leaves the above threshold state in the ON phase (i.e., the first state starts and finishes with an error-free burst), whereas it always reaches/leaves the below threshold state in the OFF phase (i.e., the second state starts and finishes with an error burst).

Once $T^{(k)}$ has been set (i.e., the threshold ϑ has been selected), each element p_{ij} of the probability transition matrix $\mathbf{P}$ can been obtained by simply counting the number of transitions from the state S_i to the state S_j, divided by the number of occurrences of the state S_i in the data trace. In the same way, the elements π_i of the state vector $\mathbf{\Pi}$ are obtained by counting the relative number of the occurrences of S_i in the data trace.

Now, considering measured data we can estimate $\Phi_i(x_F)$, $\Psi_i(x_R)$, and $\Upsilon_i(n_b^i)$ (in our simplified case $i = 1, 2$). But for the model we need to establish their best fitting distributions.

From the analysis of the error-free length distributions in Sec. 3, we highlighted the great variability of the mean, variance, and maximum of burst length. To take in account this behavior, we found that the best choice for fitting error-free burst length was a weighted sum of one logarithmic and one geometric probability mass functions (pmfs). The expression of the considered pmf, for a discrete random variable X, is:

$$p_X(n) = P(X = n) = \alpha k \frac{c^x}{x} + (1 - \alpha)p^{x-1}(1 - p), \qquad n \in N^+; \quad 0 < (c, p) < 1; \qquad (7)$$

where $k = -1/\ln(1 - c)$ and $\alpha < 1$ is the mixture weight.

The logarithmic pmf has been chosen because it shows a pronounced long-tail behavior, like the burst length distribution of several data sets (i.e., it is well suited for fitting their tails). Note that, as more the parameter c gets close to 0, more the logarithmic distribution shape gets tight and sharp around its mean value. On the contrary, when c gets close to 1, the pmf becomes flatter and shows a much marked long-tail behavior.

At the same time, with the geometric pmf we take into account the behavior of error-free burst distribution for values closer to the origin, since it has a more pronounced decay slope.

By choosing an appropriate value for α, we can consider cases of distribution tails more or less pronounced. From Fig. 11, it can be noticed that the considered distribution mix provides a very good fitting for error-free burst lengths in several scenarios (i.e., mean and max values which differs even of one order).

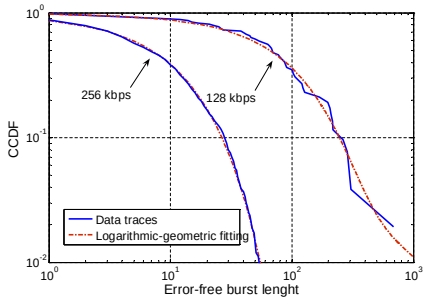

Figure 11. CCDFs of the error-free burst length for traffic flows at 128 kbps and 256 kbps (interference on ch. 1).

Since values of error burst length distributions show a very lower variability (i.e, in the range from 3 up to about 15 frames), it is sufficient to use one logarithmic distribution to obtain a good fitting for both the functions $\Psi_1(x_R)$ and $\Psi_2(x_R)$.

For what concerns the best fitting distributions for Nb^1 and Nb^2, the main difficulty is that such distributions change as the threshold ϑ_1 changes. After some analysis on our data set, we found that the best pmf to account for this behavior and to fit both $\Upsilon_1(n_b^1)$ and $\Upsilon_2(n_b^2)$ was a discretized version of the Inverse Gaussian distribution, also known as Wald distribution [30], which pmf is:

$$p_X(n) = P(x_{n-1} < X \leq x_n) = \int_{x_{n-1}}^{x_n} \sqrt{\frac{\lambda}{2\pi\tau^3}} e^{\lambda(\tau-\mu)^2/(2\tau\mu^2)} d\tau, \qquad n \in N^+,\ \mu > 0,\ \lambda > 0 \tag{8}$$

where μ is the mean and λ is the scaling parameter.

We point out that the distributions selected above are effective for the considered measured data set. In fact, changing data sets requires a new characterization of distributions, but the general k-TM framework remains still valid.

5.2. The Maximum Likelihood Estimators

To estimate the unknown parameters of the considered distributions, we used a general parameter estimation technique: the Maximum Likelihood Method (MLM). It is well know that the ML estimators are efficient for large samples and they are asymptotically normal,

unbiased, and with minimum variance [12]. The technique works considering the joint density function of n observation x_i, from the random variable X, as dependent from the vector of unknown parameters θ. Hence, the estimation problem it is reduced to the maximization of the so called *Log-likelihood function* (see [12] for the details). Applying the MLM to (8), we obtain the following closed form expression:

$$\hat{\mu} = \bar{x}, \qquad 1/\hat{\lambda} = \frac{1}{n}\left(\sum_{i=1}^{n} x_i^{-1} - \hat{\mu}^{-1}\right); \tag{9}$$

where n is the sample size, $\overline{x}$ is the sample mean, $\hat{\mu}$ and $\hat{\lambda}$ are the ML parameter estimates of the Wald distribution.

For both the logarithmic distributions, which fit the error burst length distributions in the two states, we obtain:

$$\overline{x_i} = \frac{\hat{c_i}}{-(1-\hat{c_i})\ln(1-\hat{c_i})}, \qquad i \in [1,2]; \tag{10}$$

where $\overline{x_i}$ is the mean value of the error burst length and $\hat{c_i}$ is the ML estimation of the logarithmic parameter. Eq. (10) can be easily solved with any numerical method.

Finally, applying the MLM to the logarithmic-geometric mix in Eq.(7), we obtain a non-linear system of three equations (each one from the partial derivative with respect to c, α and p) that can be solved by using numerical tools such as those implementing the Reflective Newton Methods [31].

6. Numerical Results

The performance of an error model can be valuated by means of two different procedures. In the first one, statistics are calculated directly from the model by means of analytic expressions. In the second one, artificial error traces are generated using the models and the statistics are evaluated from these synthetic traces. In this paper, we follow the latter procedure since analytical expressions cannot be easily obtained for all the considered models.

6.1. Trace generation from models

To obtain synthetic traces using the considered models, we follow a three step procedure: (i) define the order of each model, (ii) establish the trace lengths, (iii) generate the artificial traces.

It is important to note that we are considering Markovian models. Thus, the order is directly related to the computational complexity of the model as discussed in previous papers [6, 7, 14]. Therefore, the results reported below about the order of the considered models can be seen as an indirect measure of their computational complexity.

To assess the order of each model, all the measured data traces have been considered. In particular, for the models based on Markov chains (i.e., the k-th order FSMC, the MTA, and the M^3) the condition in eq. (4) has been used; for the Extended ON/OFF model, the number of phases has been chosen to better fit error and error-free burst CCDFs as in [3]; finally, for the threshold model, two states (i.e., four phases) have been always used.

Tab.I summarizes results for the considered models in all the transmission conditions and interference scenarios. In particular, each value represents the average of the model orders

obtained applying the considered model to all the data traces. For this reason, some values are not integer as expected.

Table I. Average order of the considered models.

Type of Flow	*Interfering Channel*	*k-th order FMSC*	*MTA*	M^3 M^3		*Extended ON/OFF*		*2-state threshold*
				lossy state	*hidden state*	*ON phases*	*OFF phases*	*# states (# phases)*
128 kbps	Ch. 1	5	1.90	1.90	2.50	1	2.75	2 (4)
	Ch. 2	5	3.70	3.70	4.00	1	2.30	2 (4)
	Ch. 3	5	4.20	4.20	4.00	1	2.40	2 (4)
256 kbps	Ch. 1	5	2.20	2.20	3.70	1	2.70	2 (4)
	Ch. 2	5	3.90	3.90	4.00	1	2.10	2 (4)
	Ch. 3	5	4.50	4.50	3.90	1	2.90	2 (4)
512 kbps	Ch. 1	5	2.50	2.50	4.00	1	2.80	2 (4)
	Ch. 2	5	4.20	4.20	4.00	1	2.10	2 (4)
	Ch. 3	5	4.70	4.70	3.80	1	3.00	2 (4)
VoIP	Ch. 1	5	2.50	2.50	3.60	1	2.70	2 (4)
	Ch. 2	5	3.50	3.50	4.00	1	2.50	2 (4)
	Ch. 3	5	5.00	5.00	4.00	1	3.00	2 (4)

It is interesting to notice that for the k-th order FSMC models the chain order is always equal to 5 regardless to the interference level and to the sources transmission rate. Whereas, in both the cases of M^3 and MTA models, the order of the FSMCs, which they are based on, increases with the interference level as well as with the transmission rate. Furthermore, the average order of the FSMCs in the MTA model is less or equal to 5, that means it is cheaper than the simpler 5-th order FSMC model. Nevertheless, in the M^3 algorithm the use of FSMCs for modeling transitions among hidden states quite double the overall model order. Finally, only a smooth variation with both transmission rate and interference level can be noticed for the number of OFF phases in the Extended ON/OFF model. It is important to stress that, for a Markov model, the order is directly related to its computational complexity. Thus, the complexity of the proposed new k-TM model can be kept low considering a few number of states; numerical results will show that this does not reduce effectiveness of our approach.

The second step in synthetic trace generation is the choice of trace lengths. A good tradeoff between time spent and reliability of results is to run the simulation for about 20 times the experimental data set length. In this manner, synthetic traces of about half million of frames have been obtained for each data set using all the considered models.

Traces generation for M^3 and MTA models proceeds following the algorithm shown in [9]. Besides, for both the k-th order FSMC and the Extended ON/OFF model, after having randomly chosen the initial state accordingly to the asymptotic probability state vector, the next chain states have been found following the transition probability matrix.

Finally, fixed the number N of synthetic trace frames and the threshold value, the Algorithm 1 (see below) has been used for the 2-state threshold model. Note that to generate the lengths t_a, t_b, x_F, and x_R, we used the inverse transformation method [12].

```
Set State using probability vector Π; while Number of synthetic frames generated ≤ N do
    if in the Above threshold state then
        Set Above threshold subtrace length, L_A = 0; x_R = x_F = 0;
        Generate t_a (sojourn time expressed in frames) using the inverse CDF of r.v. N_b^1;
        while L_A < t_a do
            Generate an error-free burst of x_F frames, using the inverse CDF of r.v. X_F;
            L_A = L_A + x_F + x_R;
            if L_A < t_a then
                Generate an error burst of x_R frames, using the inverse CDF of r.v. X_R;
            end
        end
        Set State = "Below threshold"

    else if in the Below threshold state then
        Set Below threshold subtrace length, L_B = 0; x_R = x_F = 0;
        Generate t_b (sojourn time expressed in frames) using the inverse CDF of N_b^2;
        while L_B < t_b do
            Generate an error burst of x_R frames, using the inverse CDF of X_R;
            L_B = L_B + x_R + x_F;
            if L_B < t_b then
                Generate an error-free burst of x_F frames, using the inverse CDF of X_F;
            end
        end
        Set State = "Above threshold"
    end
    Link together the two subsequences;
end
```

Algorithm 1: Pseudo-code for generation of k-TM trace frame, with $k = 2$.

6.2. Performance metrics

Some metrics have been introduced in order to assess performance of the considered models with reference to first and second order error statistics defined by eqs. (1)-(3). We consider:

- The FER estimation relative error:

$$RE_{fer} = |FER_t - FER_m|/FER_t \tag{11}$$

  where FER_t and FER_m are the frame error rates estimated from measured data traces and synthetic traces, respectively.
- The mean CCDF estimation relative error (for both error and error-free burst):

$$RE_{ccdf} = \frac{1}{n_c}\sum_{i=1}^{n_c} |F_t^{(c)}(i) - F_m^{(c)}(i)|/F_t^{(c)}(i), \tag{12}$$

  where $F_t^{(c)}(\cdot)$ and $F_m^{(c)}(.)$ are the burst CCDFs estimated from measured data traces and synthetic traces, respectively; and n_c is the number of percentiles in the data trace.
- The mean autocorrelation coefficient relative error:

$$RE_{\rho} = \frac{1}{n_{\rho}}\sum_{i=1}^{n_{\rho}} |\rho_t(i) - \rho_m(i)|/\rho_t(i), \tag{13}$$

  where $\rho_t(h)$ and $\rho_m(i)$ are the autocorrelation coefficients estimated from measured data traces and synthetic traces, respectively; n_{ρ} is the minimum between h_{max} and 1000; and $h_{max} = max\{h|\rho_t(h) > c_b\}$ with c_b equal to the confidence bound for the autocorrelation at the significance level $\alpha = 0.01$.

The upper bound n_ρ in the sum (13) is chosen in order to assess autocorrelation fitting performance at most up to 1000 lags, but in any case not above the limit given by the confidence bound. The threshold value, ϑ_1, in the 2-state threshold model has been chosen in order to minimize autocorrelation coefficient relative error given by eq. (13), that is, to improve the model capability to fit the trace autocorrelation structure.

Fig. 12 reports the mean FER estimation relative error for the five compared models, using eq. (11). Results refer to all the interference scenarios and transmission rates. It can be noticed that only the MTA model shows bad performance in capturing traces FER, especially for transmissions in better interference conditions (i.e., when interference is on channel 1), where RE_{fer} is about 16%. The other models, instead, show very good agreement with trace FERs; indeed, RE_{fer} is always in the range $= 2\% \div 3\%$. In particular, for the k-TM model, RE_{fer} is always less then 2%. Moreover, the FER estimation relative error does not depend on the transmission rate and on the interference level. This proves the model capability in capturing the FER in different operational conditions.

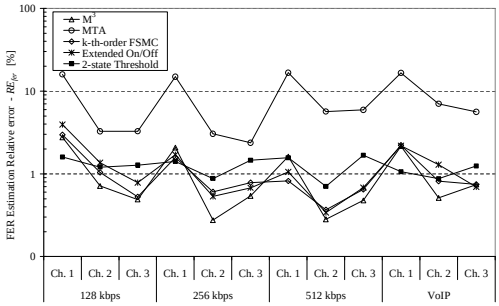

Figure 12. Mean FER estimation relative error, by means of models and traces.

Concerning fitting performance for error-free burst, results obtained by eq. (12) have been reported in Fig. 13. It is worth noticing that all the models, for the same source transmission rate, get worst in fitting the long tail distributions when in the presence of interference on channel 1. Furthermore, for the 2-state threshold model, RE_{ccdf} is always about 3% (and often about 1%); that is, it provides better performance. For the M^3 it can be noticed that its increased complexity is not always consistent with performance enhancements either in comparison with the 5-th order FSMC and the MTA model. Finally, despite the Extended ON/OFF model uses up to 3 or 4 phases to fit length distributions of error-free bursts, it does not achieve the same performance of the 2-state threshold model which uses only a mix of one geometric and one logarithmic distribution. In particular, this is true for interfering transmission on channel 1 (see Fig. 13).

From Fig. 14, which reports the values of RE_{ccdf} for the error burst length, it can be noticed that all the models show a very good behavior referring to this metric. However, minor performance has been obtained in fitting error burst length distribution of VoIP transmission in low interference conditions (i.e., interference on channel 1), with the exception of the 2-state threshold model which RE_{ccdf} index is always about 0.2%. It is interesting to notice that the 5-th order FSMC performance is very close to the 2-state threshold model one, and in any case it is better than the ones of the other models.

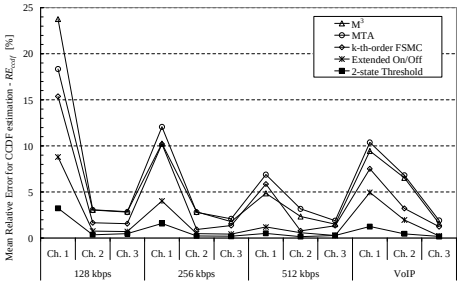

Figure 13. Mean relative error for CCDF of error-free burst length, estimated by means of models and traces.

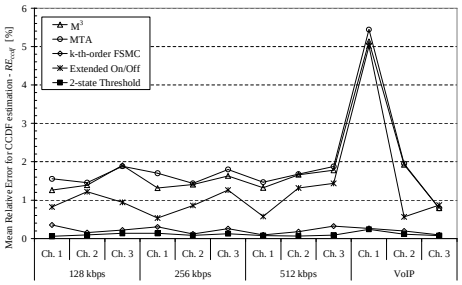

Figure 14. Mean relative error for CCDF of error burst length, estimated by means of models and traces.

Finally, Fig. 15 shows the average values of the autocorrelation relative error RE_ρ. It is easy to understand why RE_ρ shows an increasing trend both with interference level and with the transmission rate, recalling the results reported in Sec. 3 on the relationship among such parameters and the time scale extension of the autocorrelation coefficient. In fact, the number of lags for which the autocorrelation is significantly different from zero rises as either interference levels or transmission rates grow. Thus, the index RE_ρ will account for the autocorrelation mismatch over a longer time-scale. Moreover, it can be noticed that M^3 and MTA models perform bad and RE_ρ assumes very similar values. Slightly better, but not satisfactory, results have been obtained for both the 5-th order FSMC and for the Extended ON/OFF model. For the 2-states threshold model, instead, better results have been obtained since RE_ρ values are almost halved in comparison with the corresponding ones of any other model. Nevertheless, for the threshold model, further performance improvement can be obtained by using much more states (i.e., more thresholds), and by accounting for a larger number of error paths in the original sample traces. Although it comes with a major complexity.

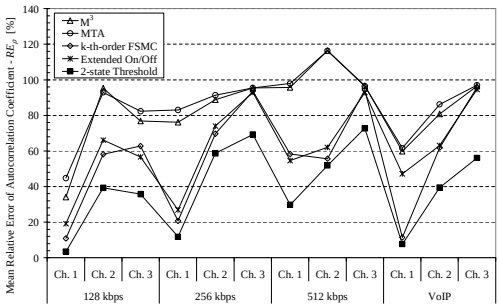

Figure 15. Mean relative error of autocorrelation coefficients, estimated by means of models and traces.

From the afore discussion, it can be concluded that the proposed new k-TM model has capabilities similar to the other models in capturing data traces FER, but it is significantly better than the others in fitting both error and error-free burst length distributions. Moreover, it makes a significant step further in the challenging issue of capture the autocorrelation

structure of error traces. Finally, we point out that the 2-states threshold model is the only one showing consistent performance for all the considered metrics.

7. Conclusions

In this paper a comprehensive measurements campaign in a 802.11 based wireless area network has been performed, considering different transmission rates and simulating variable channel interference levels. The obtained results were statistically analyzed highlighting FER, error and error-free burst length CCDFs and the autocorrelation coefficient. Therefore, a new wireless model for channel errors at link layer, referred to as k-TM (k-state threshold model), has been introduced and its 2-state instance has been investigated in 802.11 channel modeling.

The proposed model has been compared with four models already in literature: the k-th order FSMC, the M^3, the MTA, and the Extended ON/OFF model. Results show that the proposed new model captures extremely well (often better than the other ones) trace first order statistics, such as FER and error and error-free burst length CCDFs, in all the interference conditions and for all the transmission rates. Moreover, it performs better than the other in capturing data traces autocorrelation; such a result can be further improved by increasing the number of states.

Finally, the implementation cost of the proposed algorithm is appreciably lower than the other ones since it requires few states and variables to be estimated. Nevertheless, it requires some preliminary investigation to better fit the distributions of both the states sojourn time, and the error/error-free burst length distributions.

In future works, we intend to investigate the performance of the proposed model considering other 802.11 traces available in the scientific community. Hence, we will extend the analysis to the errors at bit level. Moreover, we want to compare our approach with some promising non-Markovian approaches; in particular, we will consider models based on Chaotic Maps, which are particularly suitable for matching error/error-free burst distributions with extremely long-tails.

REFERENCES

1. Rappaport TS. *Wireless Communications, principles and practice*. 2 edn., Prentice Hall PTR, 2002.
2. Khayam S, Karande S, Radha H, Loguinov D. Performance analysis and modeling of errors and losses over 802.11b lans for high-bitrate real-time multimedia. *Signal Processing: Image Communication* August 2003; **18**:575–595.
3. Ji P, Liu B, Towsley D, Kurose J. Modeling Frame-level Errors in GSM Wireless channels. *Performance Evaluation* Jan 2004; **55**(1-2).
4. Konrad A, Zhao BY, Joseph AD, Ludwig R. A Markov-based Channel Model Algorithm for Wireless Networks. *Wireless Networks* May 2003; (9):189–199.
5. Arauz J, Krishnamurthy P. Markov modelling of 802.11 channels. *Proc. of IEEE VTC'03-Fall*, Orlando, FL, 2003.
6. Konrad A, Zhao BY, Joseph AD, Ludwig R. A Markov-based channel model algorithm for wireless networks. *Proc. of Fourth ACM International Workshop on Modeling, Analysys and simulation of wireless and mobile systems*, Rome, Italy, 2001.
7. Khayam SA, Radha H. Markov-based modeling of wireless local networks. *Proc. of ACM MSWiM'03*, San Diego, California, USA, 2003.
8. Khayam SA, Radha H. Analysis and modeling of errors at the 802.11b link layer. *Proc. of IEEE ICME*, Baltimore, Maryland, USA, 2003.

9. Konrad A, Joseph AD. Choosing an accurate network path model. *Proc. of ACM SIGMETRICS*, San Diego , CA, USA, 2003.
10. Boggia G, Buccarella D, Camarda P, D'Alconzo A. A simple on/off logarithmic model for frame-level errors in wirekess channel applied to gsm. *Proc. of IEEE VTC'04-Fall*, Los Angeles, 2004.
11. Kleinrock L. *Queuing Systems, Vol. 2nd: Computer Applications*. Wiley & Sons, 1985.
12. Papoulis A. *Probability, Random Variables and Stochastic Processes*. 3 edn., Mc Graw Hill, 1991.
13. Ji Z, Li BH, Wang HX, Chen HY, Sarkar TK. Efficient ray-tracing methods for propagation prediction for indoor communications. *IEEE Antennas Propagation* April 2001; **43**(7):41–49.
14. Zorzi M, Rhao RR, Milstein LB. On the accuracy of a first-order Markov model for data block transmission on fading channel. *Proc. of IEEE VTC'97*, 1997; 1528–1532.
15. Wang HS, Chang PC. On verifying the first-order Markovian assumption for a Rayleigh fading channel model. *Transaction on Vehicular Technology* March 1996; **45**:349–356.
16. Pimentel C, Falk TH, Lisboa L. Finite-state Markov modeling of correlated Rician-fading channels. *IEEE Transactions on Vehicular Technology* September 2004; **53**(5):1491–1501.
17. Tan CC, Beaulieu NC. On first order Markov models for the Rayliegh fading channel. *Transaction on Communications* December 2000; **48**(12):2032–2040.
18. Zorzi M, Rao RR, Milstein LB. Error statistics in data transmission over fading channels. *Transaction on Communications* November 1998; **46**(11):1468–1476.
19. Jiao C, Schwiebert L, Xu B. On modeling the packet error statistics in bursty channels. *Proc. of 27th Annual IEEE Conference on Local Computer Networks (LCN'02)*, Tampa, FL, 2002.
20. Nguyen GT, Katz R, Noble B. A trace-based approach for modeling wireless channel behavior. *Proc. of the Winter Simulation Conference*, Coronado, FL, 1996; 597–604.
21. Rabiner LR. A tutorial on hidden Markov models and selected applications in speech recognition. *Proc. of IEEE* Feb 1999; **2**(2):257–286.
22. Salamatian K, Venton S. Hidden Markov modeling for network communication channels. *ACM Sigmetrics Performance Evaluation Review* 2001; .
23. Hartwell JA, Fapojuwo AO. Modeling and characterization of frame loss process in ieee 802.11 wireless local area networks. *Proc. of IEEE VTC'04-Fall*, Los Angeles, 2004.
24. Willing A. A new class of packet and bit-level models for wireless channels. *Proc. of IEEE PIMRC'02*, Lisboa, Portugal, 2002.
25. Kopke A, Willig A, Karl H. Chaotic maps as parsimonious bit error models of wireless channels. *Proc. of IEEE Infocom 2003*, S.Francisco, CA, 2003; 597–604.
26. International Telecommunication Union (ITU). *Reduced complexity 8 kbit/s CS-ACELP speech codec*. ITU-T Recommendation G.729, Annex A Nov 1996.
27. IEEE 80211. *Information Technology - Telecommunications and Information Exchange between Systems Local and Metropolitan Area Networks Specific Requirements Part 11: Wireless LAN Medium Access Control (MAC) and Physical Layer (PHY) Specifications*. ANSI/IEEE Std. 802.11, ISO/IEC 8802-11, first edn. 1999.
28. Brockwell PJ, Davis RA. *Introduction to Time Series and Forecasting*. Springer, 1996.
29. Merhav N, Guntman M, Ziv J. On the estimation of the order of a Markov chain and universal data compression. *IEEE Transaction on Information Technology* September 1989; **35**(5):1014–1019.
30. Evans M, Hastings N, Peacock B. *Statistical Distributions*. 3 edn., John Wiley & Sons, Inc., 2000.
31. Coleman TF, Li Y. On the convergence of reflective Newton methods for large-scale nonlinear minimization subject to bounds. *Mathematical Programming* 1994; **67**(2):189–224.